



Universiteit  
Leiden  
The Netherlands

## Small molecule inhibitors of Nicotinamide N-Methyltransferase (NNMT)

Gao, Y.

### Citation

Gao, Y. (2021, September 29). *Small molecule inhibitors of Nicotinamide N-Methyltransferase (NNMT)*. Retrieved from <https://hdl.handle.net/1887/3213827>

Version: Publisher's Version

License: [Licence agreement concerning inclusion of doctoral thesis in the Institutional Repository of the University of Leiden](#)

Downloaded from: <https://hdl.handle.net/1887/3213827>

**Note:** To cite this publication please use the final published version (if applicable).

# Chapter 6

---

## Summary

## SUMMARY

The function of NNMT in healthy and disease states has gained increased attention in recent years. Overexpressed levels of NNMT have been observed in various cancers, and increased NNMT expression has been related to tumour progression, metastasis, and worse clinical outcomes. NNMT is considered to be a new potential pharmacological target in the treatment of a variety of cancers, metabolic disease and other pathologies. The growing number of publications elucidating the role of NNMT in disease has in turn spurred the development of potent and selective inhibitors of NNMT with an increasing number of compounds being disclosed in the past five years.

**Chapter 1** provides a comprehensive review of the current status of NNMT inhibitor development, relevant *in vitro* and *in vivo* studies, and a discussion of the challenges faced in the development of NNMT inhibitors. Although the search for effective NNMT inhibitors is still in its infancy, substantial achievements have been made in identifying potent and selective small-molecule inhibitors of NNMT. That said, the limited cellular and *in vivo* activity of these compounds speak to the need to develop more drug-like inhibitors. The clinical importance of NNMT in various diseases, including cancer and metabolic disorders, support it as a promising therapeutic target. However, there are many limitations in the currently available set of NNMT inhibitors. The adenosine and amino acid moieties of the SAM mimetics are considered critical moieties in NNMT inhibitors. While these features are crucial for activity, they also negatively affect cell permeability. To assess the therapeutic viability of NNMT inhibition in more detail, the current set of NNMT inhibitors available needs to be expanded to provide more drug-like molecules.

In **chapter 2**, a diverse library of inhibitors was prepared to probe the different regions of NNMT's binding site. To this end, various structural motifs were explored for their ability to improved potency and binding within the NNMT binding pocket. Among the bisubstrate analogues prepared, the most potent NNMT inhibitor was found to be naphthalene-containing compound **78**, displaying an  $IC_{50}$  value of 1.41  $\mu M$ , >10-fold better than its parent compound MvH45 (compound **1** in **chapter 2**). From modelling studies, the improved activity of compound **78** can be rationalized by the apparent presence of an intramolecular hydrogen bonding interaction predisposing the compound to an active conformation with lower entropic cost. In addition, the modelling indicates

that the naphthalene group in **78** is appropriately oriented to benefit from additional  $\pi$ – $\pi$  stacking interactions with several tyrosine residues in the nicotinamide binding pocket of NNMT. (Figure 1). The cellular data obtained for compound **78** show a dose-dependent effect on cell proliferation in HSC-2 oral cancer cells.

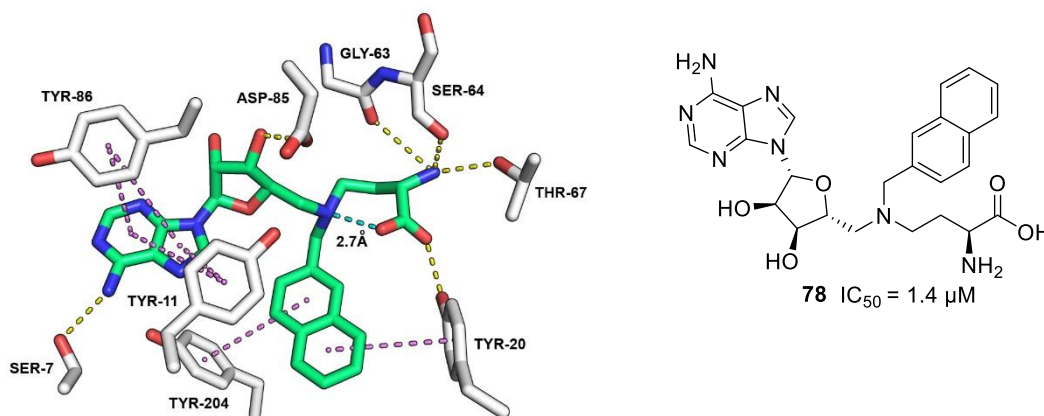


**Figure 1.** Modelling results for compound **78** in the NNMT active site (PDB ID: 3ROD). Molecular dynamics simulation indicates the presence of an intramolecular hydrogen bond (2.7Å, shown in cyan) specific to compound **78** (in green)

**Chapter 3** reports a scaffold-hopping strategy to generate novel and potent bisubstrate NNMT inhibitors (**17o**, **17r**, **17u**, Figure 2). The inhibition data of the inhibitors thus prepared revealed a striking effect for electron-withdrawing groups present on the aromatic ring, predominantly when introduced at the position *para* to the alkene linker. Among these compounds, the *para*-cyano substituted styrene-based inhibitor **17u** was identified as the most potent NNMT inhibitor with an  $IC_{50}$  value of 3.7 nM. These studies demonstrated that minor changes in the amino acid side chain and adenosine moiety lead to remarkable decreases in potency. Modelling studies predict the presence of hydrogen bonding interactions between the *para*-cyano group and two active site serine residues in the nicotinamide binding pocket of NNMT, providing a possible explanation for the potency of compound **17u**. Notably, the potent inhibition exhibited by **17u** in biochemical assays was not observed in cell-based assays; only when tested at a very high concentration of 100  $\mu$ M was a decline in cell viability observed for oral, lung, and bladder cancer cell lines treated with the compound.

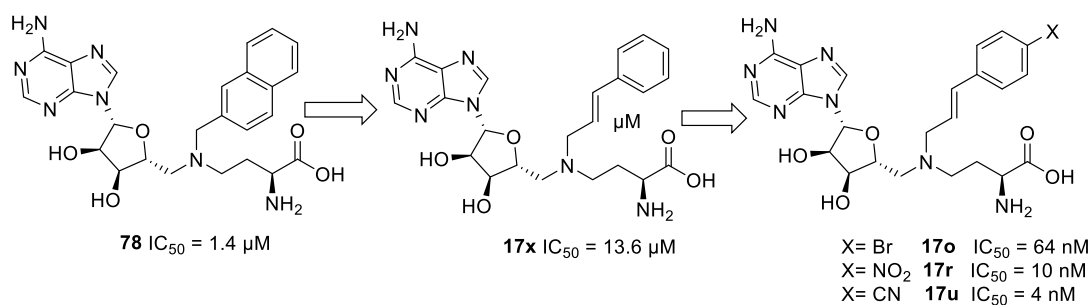


**Figure 2.** Scaffold-hopping strategy to generate novel and potent bisubstrate inhibitors.

In **chapter 4** a prodrug strategy is described to decrease the polarity of compound **17u** and improve its cellular activity. Specifically, the carboxylic acid on inhibitor **17u** was masked as an ester using a variety of alkyl and benzyl groups, and the amine moiety was masked using the trimethyl-lock (TML) group. The different combinations of esterase-cleavable prodrugs thus prepared lead to the selection the isopropyl prodrug **12e** and the isopropyl-TML dual-prodrug **14e** (Figure 3) as the compounds with the most promising profile in terms of stability and cellular activity. Initially, the compounds were tested in an MTT cell viability assay using three different cancer cell lines, but cellular activity was observed only at the highest concentration of 100  $\mu M$  tested. Subsequently, a cellular MNA determination assay was performed, revealing a dose-dependent effect of NNMT prodrug inhibitors **12e** and **14e** on MNA levels in cells, with significant improvement over the parent compound. The data presented here demonstrate the suitability of a prodrug strategy to deliver polar NNMT inhibitors into cells.

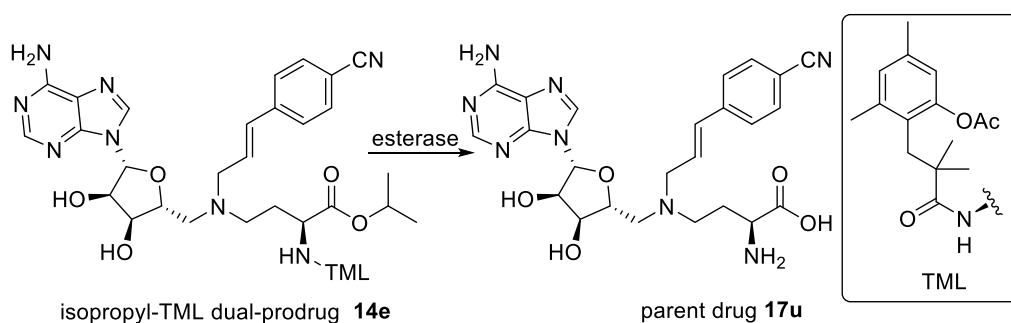


**Figure 3.** Prodrug **14e** hydrolysis to form parent drug **17u**.

In **chapter 5**, the design and synthesis of a library of compounds is described that aim to covalently target active site cysteine and serine residues using a variety of different

warheads. To do so, the amino acid sidechain in the potent NNMT inhibitor **17u** (identified in chapter 3) was replaced by an acrylamide or chloroacetamide warhead with different linkers to target cysteine residues C159 and C165, for which covalent inhibitors have been described previously. The most active compound (**17b**, Figure 4) thus prepared showed an  $IC_{50}$  value of 400 nM, making it the first example of a bisubstrate inhibitor in which the amino acid sidechain was successfully replaced without rendering it inactive. In another approach, the cyano group of compound **17u** was replaced by either a sulfonyl fluoride or a boronic acid moiety with the aim of targeting serine residues S201 or S213 present in the nicotinamide pocket of NNMT. These efforts lead to potent NNMT inhibition by *meta*- and *para*-sulfonyl fluoride compounds **39a** ( $IC_{50}$  = 89 nM) and **39b** ( $IC_{50}$  = 68 nM, Figure 4). Interestingly, the significant difference in activity observed for *meta*- versus *para*-substitution, discussed in chapter 3, was not observed for the sulfonyl fluorides. The boronic acid compounds revealed moderate activity for the *meta*-substitution with no inhibition observed for *para*-substituted boronic acid. Modelling data of compounds **39a-b** suggest that the distance of 2.9 and 3.4 Å between the sulfonyl fluoride group and the hydroxyls of serine residues S201 and S213 could allow for a covalent interaction. Studies to reveal the mechanism of action of compounds **17b**, **39a** and **39b** are ongoing.

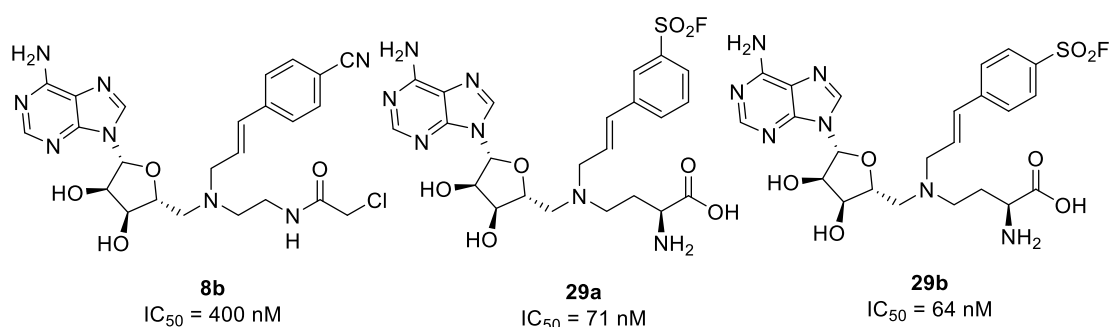


**Figure 4.** Structures of **17b**, **39a** and **39b**.

